


Cite this: *RSC Adv.*, 2022, 12, 22476

Towards novel tacrine analogues: Pd(dppf) Cl₂·CH₂Cl₂ catalyzed improved synthesis, *in silico* docking and hepatotoxicity studies†

Aravinda Babu,^a Muthipeedika Nibin Joy,^b K. Sunil,^{id} ^{*,a} Ayyiliath Meleveetil Sajith,^{*,a} Sougata Santra,^{id} ^b Grigory V. Zyryanov,^{bc} Olga A. Konovalova,^b Ilya I. Butorin^b and Keesaram Muniraju^d

A plethora of 6-(hetero)aryl C–C and C–N bonded tacrine analogues has been made accessible by employing palladium mediated (Suzuki–Miyaura, Heck, Sonogashira, Stille and Buchwald) cross-coupling reactions, starting from either halogenated or borylated residues. The successful use of Pd(dppf) Cl₂·CH₂Cl₂ as a common catalytic system in realizing all these otherwise challenging transformations is the highlight of our optimized protocols. The analogues thus synthesized allow the available chemical space around the C-6 of this biologically relevant tacrine core to be explored. The *in silico* docking studies of the synthesized compounds were carried out against the acetylcholinesterase (AChE) enzyme. The hepatotoxicity studies of these compounds were done against complexes of CYP1A2 and CYP3A4 proteins with known inhibitors like 7,8-benzoflavone and ketoconazole, respectively.

Received 23rd May 2022
Accepted 3rd August 2022

DOI: 10.1039/d2ra03225b

rsc.li/rsc-advances

Introduction

Alzheimer's disease (AD) is a chronic and progressive neurodegenerative disease characterized by loss of memory and cognitive capacity.¹ Tacrine was the first AChE inhibitor introduced in the market for the treatment of AD. However, the poor selectivity of this drug candidate resulted in side-effects, mainly hepatotoxicity.² Current AChE inhibitors used in the treatment of AD are donepezil, rivastigmine and glutamine. However, the minor side-effects associated with these drugs further demand the development of new analogues with minimal hepatotoxicity. Efforts have been made by various researchers across the globe to design and synthesize novel tacrine analogues with minimal hepatotoxicity.³ Accordingly, modifications around the tacrine core have been performed by introducing novel functionalities in the ring and by increasing or decreasing the ring sizes.⁴ Our research was focused on utilizing the bromo group in 6-bromo tacrine as a handle to explore the available chemical space around the tacrine core.

Cross-coupling reactions (C–C and C–N) have played a pivotal role in expanding the available chemical space of a lead compound during the drug development process.⁵ The use of this highly reliable and flexible methodology for developing lead like molecules to the lead optimization stage highlights its significance in medicinal chemistry. The impact of these cross-coupling technologies can be further exemplified by their large-scale applications for accessing various clinical candidates. Recent advancements in this field have further allowed the incorporation of diverse frameworks in a biologically relevant core leading to the generation of complex molecular architectures.⁶

As a part of our research programme aimed at expanding the available chemical space around the C-6 of the tacrine core,⁷ we were interested in employing palladium mediated cross-coupling reactions to synthesize novel acetyl cholinesterase inhibitors. The use of 6-bromo tacrine as a handle (for Suzuki–Miyaura, Stille, Heck, Sonogashira and Buchwald cross-coupling) was explored to furnish these novel analogues around this biologically relevant core. Several notable advances in the field of developing novel catalytic systems has led to various benefits such as increased substrate scope, milder reaction conditions, low catalyst loading *etc.*⁸ Despite the development of an array of electronically and sterically demanding catalytic systems, the need for different catalysts for various types of cross-coupling reactions still remains as a major hurdle. The use of diverse electronically and sterically demanding catalysts for successful cross-coupling reactions of a common electrophile with distinctive nucleophilic coupling partners is a major challenge prevailing in this field.⁹ Accordingly, our research was focussed on developing a common catalytic system for the cross-coupling of 6-bromo tacrine with various

^aDepartment of Chemistry, SSIT, Sri Siddhartha Academy of Higher Education, Tumkur, Karnataka, India-572107. E-mail: sunilk999@gmail.com; sajjithmeleveetil@gmail.com; Tel: +91-9480146151

^bInstitute of Chemical Technology, Ural Federal University, 19 Mira Street, Yekaterinburg, Russia-620002

^cI. Ya. Postovskiy Institute of Organic Synthesis, Ural Division of the Russian Academy of Sciences, 22 S. Kovalevskoy Street, Yekaterinburg, Russia-620219

^dGovernment Degree College-Puttur (Affiliated to S. V. University, Tirupati), Narayanavanam Road, Puttur, Chittoor (Dt), Andhra Pradesh, India-517583

† Electronic supplementary information (ESI) available. See <https://doi.org/10.1039/d2ra03225b>

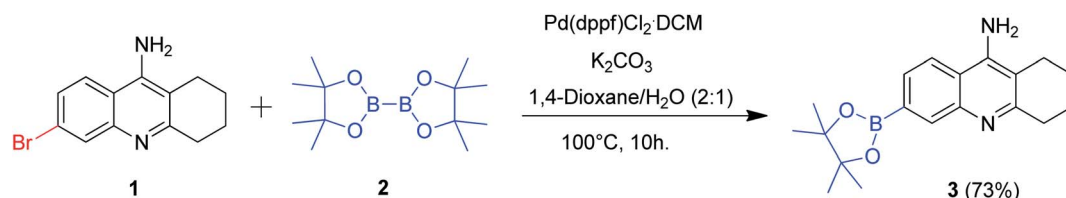


nucleophilic coupling partners (boronic acids, alkenes, alkynes and amines). In this paper, we herein report the utilization of $\text{Pd}(\text{dppf})\text{Cl}_2 \cdot \text{CH}_2\text{Cl}_2$ as a common catalyst in various palladium catalyzed cross-coupling reactions for the synthesis of diverse, pharmacologically relevant 6-substituted tacrine derivatives. The molecular docking and hepatotoxicity studies of these promising compounds were carried out at the later stage.

Results and discussion

Chemistry

The model substrate 6-bromo tacrine **1** was initially synthesized according to the previously reported procedure.^{7a} Our efforts were focussed on the cross-coupling of this model substrate with various nucleophilic coupling partners employing a common



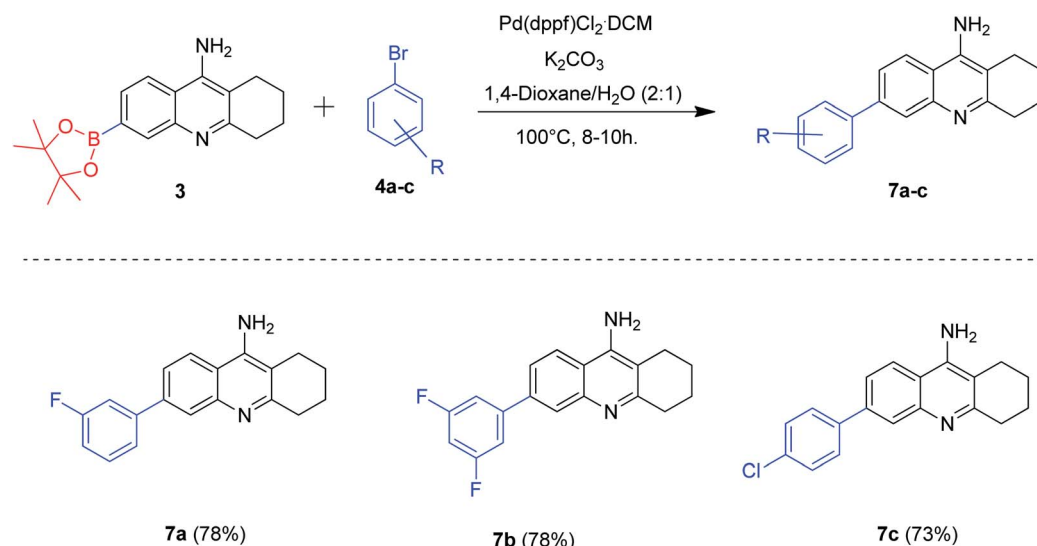
Scheme 1 Synthesis of 6-borylated tacrine derivative.

Table 1 Effect of various catalysts, bases and solvents in the borylation reaction of 6-bromo tacrine **1** with bis(pinacolonato)diboron **2**^a

Entry	Catalyst	Base	Solvent	Yield ^b 3 (%)
1	$\text{Pd}_2(\text{dba})_3$	Cs_2CO_3	DMF	Traces
2	$\text{Pd}_2(\text{dba})_3$	K_2CO_3	DMF	10
3	$\text{Pd}_2(\text{dba})_3$	CsF	DMF	Traces
4	$\text{Pd}_2(\text{dba})_3$	Na_2CO_3	DMF	8
5	$\text{Pd}(\text{dppf})\text{Cl}_2$	K_2CO_3	DMF	30
6	$\text{PdCl}_2 \cdot (\text{CH}_3\text{CN})_2$	K_2CO_3	DMF	Traces
7	$\text{Pd}(\text{OAc})_2$	K_2CO_3	DMF	Traces
8	$\text{Pd}(\text{PPh}_3)_4$	K_2CO_3	DMF	Traces
9	$\text{PdCl}_2 \cdot (\text{PPh}_3)_2$	K_2CO_3	DMF	Traces
10	$\text{Pd}(\text{dppf})\text{Cl}_2 \cdot \text{CH}_2\text{Cl}_2$	K_2CO_3	DMF	50
11	$\text{Pd}(\text{dppf})\text{Cl}_2 \cdot \text{CH}_2\text{Cl}_2$	K_2CO_3	1,4-Dioxane	60
12	$\text{Pd}(\text{dppf})\text{Cl}_2 \cdot \text{CH}_2\text{Cl}_2$	K_2CO_3	H_2O	40
13	$\text{Pd}(\text{dppf})\text{Cl}_2 \cdot \text{CH}_2\text{Cl}_2$	K_2CO_3	1,4-Dioxane– H_2O (1 : 1)	65
14	$\text{Pd}(\text{dppf})\text{Cl}_2 \cdot \text{CH}_2\text{Cl}_2$	K_2CO_3	1,4-Dioxane– H_2O (2 : 1)	73

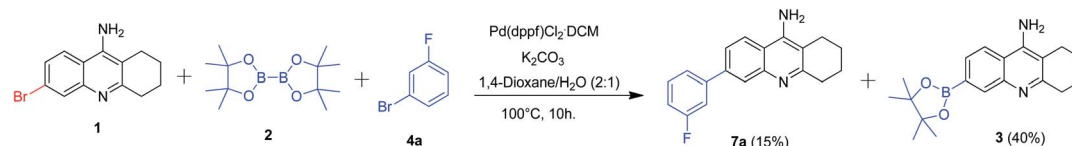
^a Reaction conditions: 6-bromo tacrine (1 mmol), bis(pinacolonato)diboron (1.5 mmol), catalyst (5 mol%), base (2.5 mmol), solvent, 100 °C for 8 h.

^b Isolated yield.



Scheme 2 Synthesis of 6-arylated tacrine derivatives by Suzuki–Miyaura coupling; reaction conditions: 6-borylated tacrine (1 mmol), aryl bromide (1.2 mmol), $\text{Pd}(\text{dppf})\text{Cl}_2 \cdot \text{CH}_2\text{Cl}_2$ (5 mol%), K_2CO_3 (2.5 mmol), 1,4-dioxane (2 mL), H_2O (1 mL), 100 °C for 8–10 h.





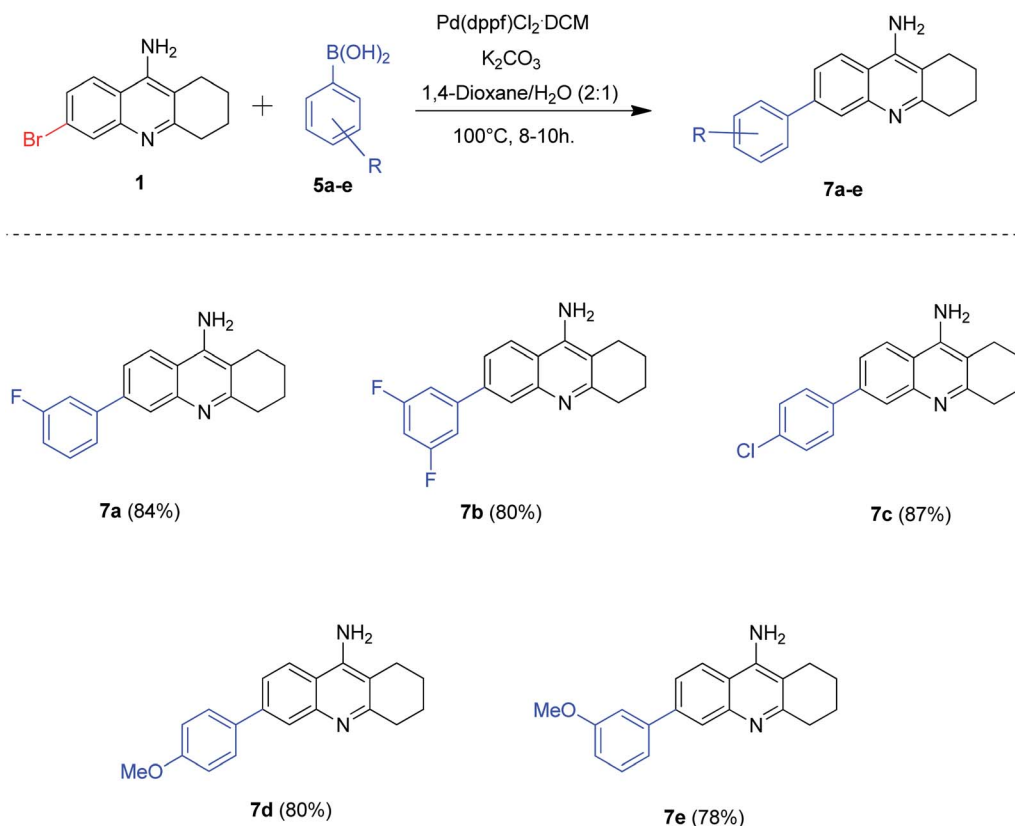
Scheme 3 One-pot protocol for borylation and Suzuki–Miyaura coupling; reaction conditions: 6-bromo tacrine (1 mmol), bis(pinacolonato)diboron (1.5 mmol), aryl bromide (1.2 mmol), Pd(dppf)Cl₂·CH₂Cl₂ (5 mol%), K₂CO₃ (2.5 mmol), 1,4-dioxane (2 mL), H₂O (1 mL), 100 °C for 10 h.

catalytic system. The presence of free amine group adds further challenges in developing a common catalytic system for this scaffold.^{7a} We started our synthetic plans by screening the palladium catalyzed borylation reaction of **1** with bis(pinacolonato)diboron **2** (Scheme 1). After the careful screening of various reaction parameters, we obtained the desired 6-boryltacrine **3** in 73% isolated yield. The detailed optimization studies for developing this methodology have been summarized in Table 1.

We screened a variety of Pd catalysts, base and solvent system so as to obtain the 6-boryltacrine in high yields (Table 1). Among the various catalysts screened, Pd(dppf)Cl₂·CH₂Cl₂ gave better results (Table 1, entries 1–10). The utilization of K₂CO₃ or Na₂CO₃ procured superior results when compared to the other bases screened (Table 1, entries 1–4). We also observed that the utilization of dual solvent system plays a pivotal role in improving the yield of the desired product (Table 1, entries 11–14). Finally, the optimized reaction conditions were affixed as

detailed in entry 14 of Table 1 since we obtained the desired product in 73% isolated yield (Scheme 1).

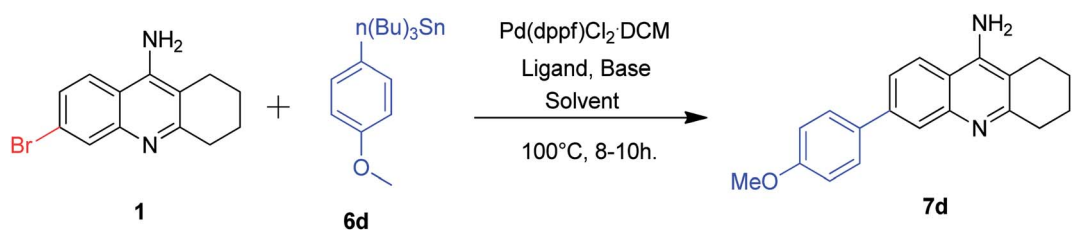
After optimizing the suitable reaction conditions for the effective borylation of 6-bromo tacrine, we directed our attention towards utilizing this boryltacrine **3** as a scaffold for the Suzuki–Miyaura cross-coupling reactions (Scheme 2). Accordingly, this intermediate **3** was treated with three different aryl bromides **4a–c** by employing the previously developed protocol of the borylation reaction. The reaction was carried out at 100 °C for 8–10 hours. Gratifyingly, all the aryl bromides reacted well enough to furnish the desired products **7a–c** in good yields. The aryl bromides having a chloro substitution at *para* position gave a slightly lesser yield (73%) of the expected product **7c** when compared to aryl bromides possessing *m*-fluoro and *m*-difluoro substituents. However, the reaction was found to be compatible for synthesizing a variety of tacrine derivatives by Suzuki–Miyaura cross-coupling conditions.



Scheme 4 Synthesis of 6-aryl tacrine derivatives by Suzuki–Miyaura coupling; reaction conditions: 6-bromo tacrine (1 mmol), aryl boronic acid (1.2 mmol), Pd(dppf)Cl₂·CH₂Cl₂ (5 mol%), K₂CO₃ (2.5 mmol), 1,4-dioxane (2 mL), H₂O (1 mL), 100 °C for 8–10 h.



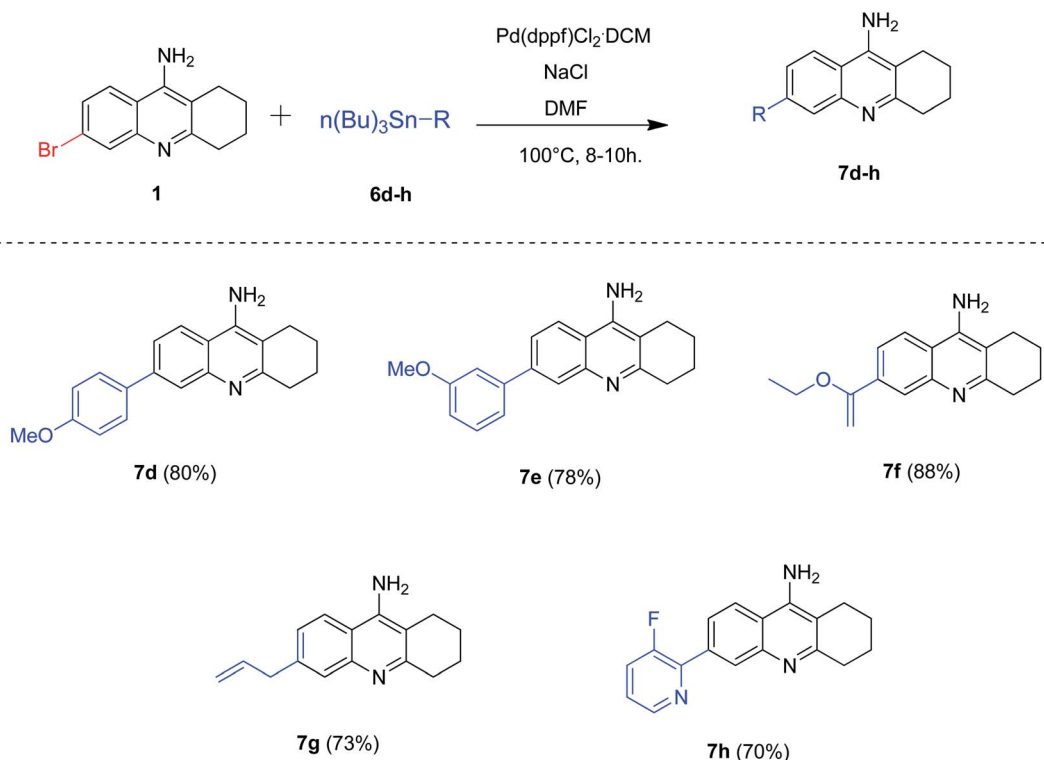
Table 2 Reaction optimization for Stille coupling reaction of 6-bromo tacrine **1** with tributyl(4-methoxyphenyl)stannane **6d**^a

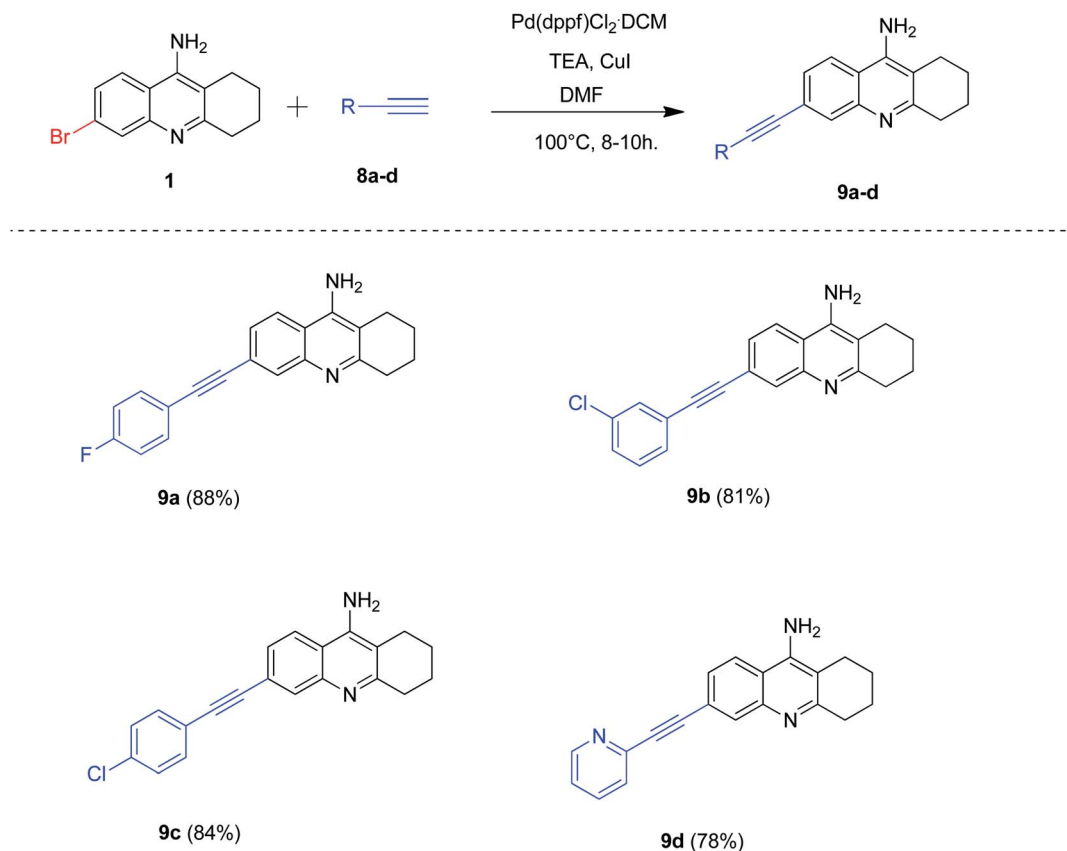
				
Entry	Catalyst	Base/additive	Solvent	Yield ^b 7d (%)
1	Pd(dppf)Cl ₂ ·CH ₂ Cl ₂	K ₂ CO ₃	1,4-Dioxane–H ₂ O (2 : 1)	40
2	Pd(dppf)Cl ₂ ·CH ₂ Cl ₂	K ₂ CO ₃	1,4-Dioxane	30
3	Pd(dppf)Cl ₂ ·CH ₂ Cl ₂	K ₂ CO ₃	H ₂ O	Traces
4	Pd(dppf)Cl ₂ ·CH ₂ Cl ₂	K ₂ CO ₃	DMF	65
5	Pd(dppf)Cl ₂ ·CH ₂ Cl ₂	Na ₂ CO ₃	DMF	60
6	Pd(dppf)Cl ₂ ·CH ₂ Cl ₂	Cs ₂ CO ₃	DMF	50
7	Pd(dppf)Cl ₂ ·CH ₂ Cl ₂	CsF	DMF	55
8	Pd(dppf)Cl ₂ ·CH ₂ Cl ₂	NaCl	DMF	80

^a Reaction conditions: 6-bromo tacrine (1 mmol), tributyl(4-methoxyphenyl)stannane (1 mmol), catalyst (5 mol%), base (1.5 mmol), solvent (2 mL), 100 °C for 8 h. ^b Isolated yield.

The aforementioned results gave us the idea of developing a one-pot protocol for borylation and Suzuki–Miyaura coupling as the developed reaction conditions was identical (Scheme 3). Accordingly, we added 6-bromo tacrine **1**, bis(pinacolonato) diboron **2** and aryl bromide **4a** along with catalyst, base and solvent and the reaction mixture was heated at 100 °C according

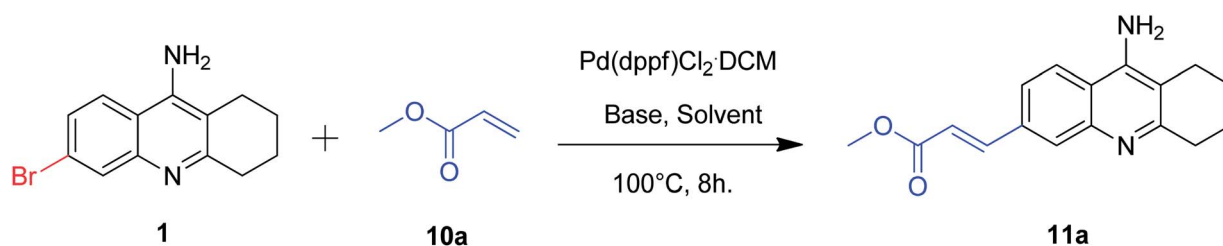
to the previously optimized protocol. Unfortunately, the desired product **7a** was obtained in 15% yield only whereas the borylated product was procured in 40% isolated yield. Hence, the one-pot protocol was not found to be effective in our optimization studies.

**Scheme 5** Synthesis of 6-substituted tacrine derivatives by Stille coupling; reaction conditions: 6-bromo tacrine (1 mmol), tributyl(aryl/vinyl) stannane (1 mmol), Pd(dppf)Cl₂·CH₂Cl₂ (5 mol%), NaCl (1.5 mmol), DMF (2 mL), 100 °C for 8–10 h.



Scheme 6 Synthesis of 6-alkynyl tacrine derivatives by Sonogashira coupling; reaction conditions: 6-bromo tacrine (1 mmol), alkyne (1.2 mmol), Pd(dppf)Cl₂·CH₂Cl₂ (5 mol%), CuI (1 mmol), TEA (2 mmol), DMF (2 mL), 100 °C for 8–10 h.

Table 3 Reaction optimization for Heck coupling reaction of 6-bromo tacrine 1 with methyl acrylate 10a^a

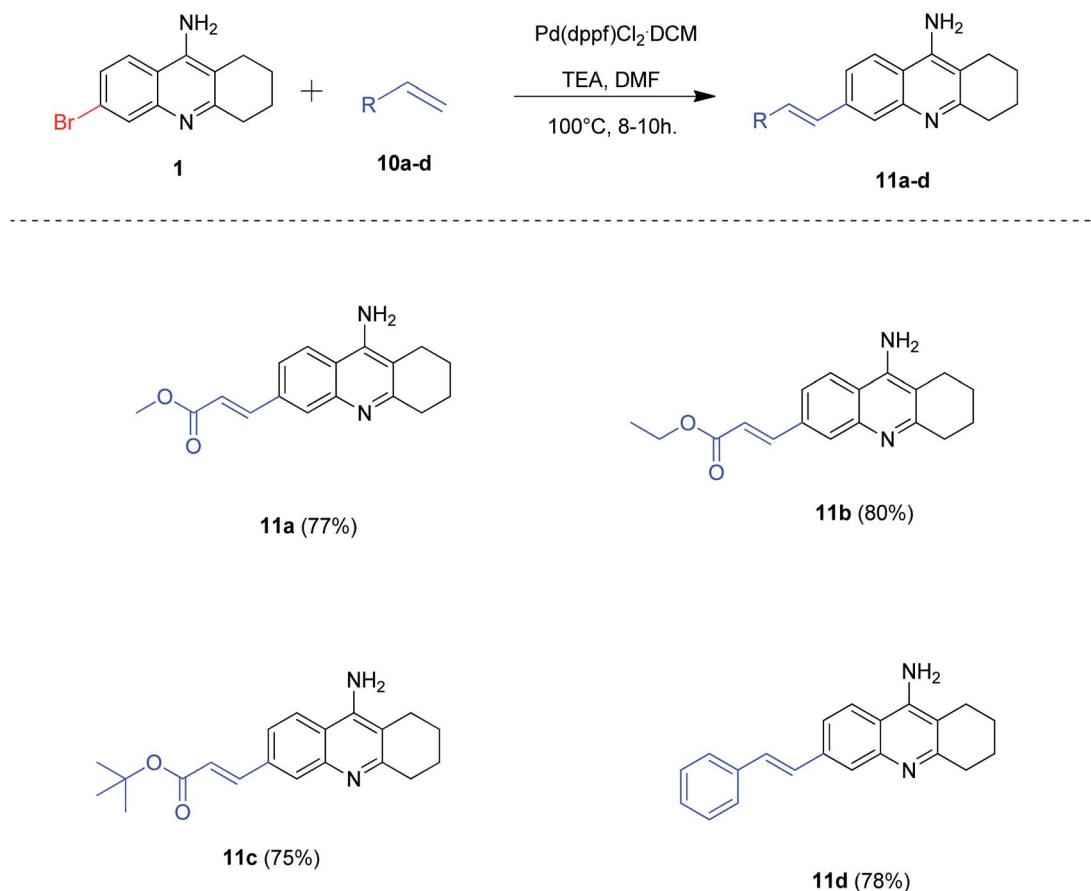


Entry	Catalyst	Base	Solvent	Yield ^b 11a (%)
1	Pd(dppf)Cl ₂ ·CH ₂ Cl ₂	K ₂ CO ₃	1,4-Dioxane–H ₂ O (2 : 1)	30
2	Pd(dppf)Cl ₂ ·CH ₂ Cl ₂	K ₂ CO ₃	1,4-Dioxane	20
3	Pd(dppf)Cl ₂ ·CH ₂ Cl ₂	K ₂ CO ₃	H ₂ O	Traces
4	Pd(dppf)Cl ₂ ·CH ₂ Cl ₂	K ₂ CO ₃	DMF	50
5	Pd(dppf)Cl ₂ ·CH ₂ Cl ₂	NaCl	DMF	45
6	Pd(dppf)Cl ₂ ·CH ₂ Cl ₂	Na ₂ CO ₃	DMF	50
7	Pd(dppf)Cl ₂ ·CH ₂ Cl ₂	Cs ₂ CO ₃	DMF	40
8	Pd(dppf)Cl ₂ ·CH ₂ Cl ₂	CsF	DMF	50
9	Pd(dppf)Cl ₂ ·CH ₂ Cl ₂	TEA	DMF	77
10	Pd(dppf)Cl ₂ ·CH ₂ Cl ₂	DIPEA	DMF	74

^a Reaction conditions: 6-bromo tacrine (1 mmol), methyl acrylate (1.2 mmol), catalyst (5 mol%), base (3 mmol), solvent (2 mL), 100 °C for 8 h.

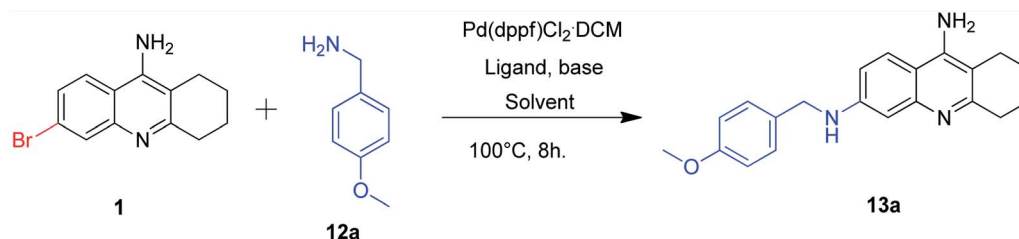
^b Isolated yield.





Scheme 7 Synthesis of 6-alkenyl tacrine derivatives by Heck coupling; reaction conditions: 6-bromo tacrine (1 mmol), alkene (1.2 mmol), Pd(dppf)Cl₂·CH₂Cl₂ (5 mol%), TEA (3 mmol), DMF (2 mL), 100 °C for 8–10 h.

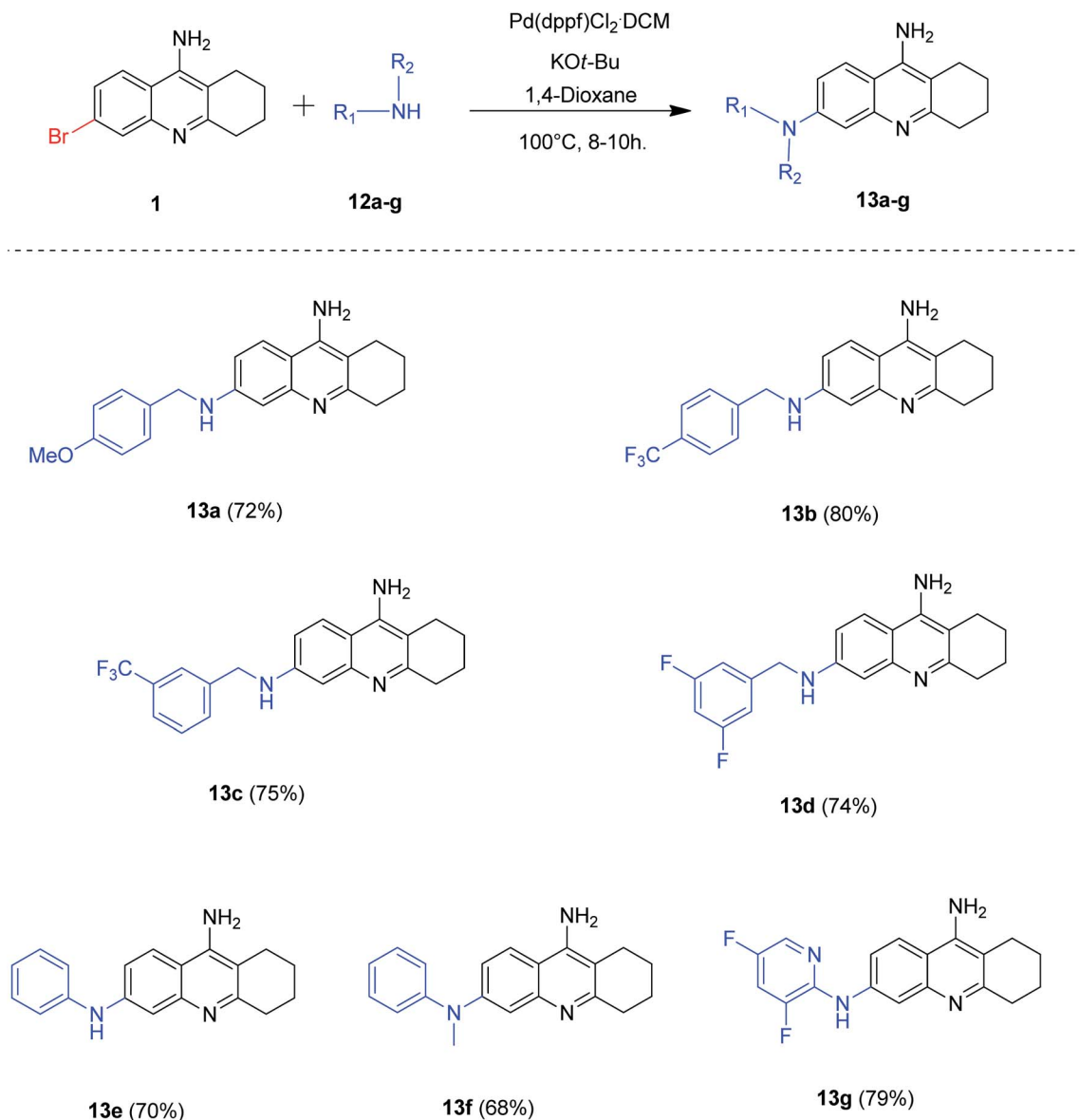
Table 4 Reaction optimization for Buchwald coupling reaction of 6-bromo tacrine **1** with 4-methoxybenzylamine **12a**^a



Entry	Catalyst	Ligand	Base	Solvent	Yield ^b 13a (%)
1	Pd(dppf)Cl ₂ ·CH ₂ Cl ₂	—	K ₂ CO ₃	1,4-Dioxane–H ₂ O (2 : 1)	5
2	Pd(dppf)Cl ₂ ·CH ₂ Cl ₂	—	K ₂ CO ₃	1,4-Dioxane	20
3	Pd(dppf)Cl ₂ ·CH ₂ Cl ₂	—	K ₂ CO ₃	DMF	15
4	Pd(dppf)Cl ₂ ·CH ₂ Cl ₂	—	Cs ₂ CO ₃	1,4-Dioxane	10
5	Pd(dppf)Cl ₂ ·CH ₂ Cl ₂	—	TEA	1,4-Dioxane	Trace
6	Pd(dppf)Cl ₂ ·CH ₂ Cl ₂	—	NaOt-Bu	1,4-Dioxane	40
7	Pd(dppf)Cl ₂ ·CH ₂ Cl ₂	—	KOt-Bu	1,4-Dioxane	65
8	Pd(dppf)Cl ₂ ·CH ₂ Cl ₂	BINAP	KOt-Bu	1,4-Dioxane	60
9	Pd(dppf)Cl ₂ ·CH ₂ Cl ₂	Xantphos	KOt-Bu	1,4-Dioxane	55
10	Pd(dppf)Cl ₂ ·CH ₂ Cl ₂	PPh ₃	KOt-Bu	1,4-Dioxane	40
11 ^c	Pd(dppf)Cl ₂ ·CH ₂ Cl ₂	—	KOt-Bu	1,4-Dioxane	72
12 ^c	Pd(dppf)Cl ₂ ·CH ₂ Cl ₂	—	KOt-Bu	DMF	67

^a Reaction conditions: 6-bromo tacrine (1 mmol), 4-methoxybenzylamine (1.3 mmol), catalyst (5 mol%), ligand (10 mol%), base (3 mmol), solvent (2 mL), 100 °C for 8 h. ^b Isolated yield. ^c 4 mmol of base used.





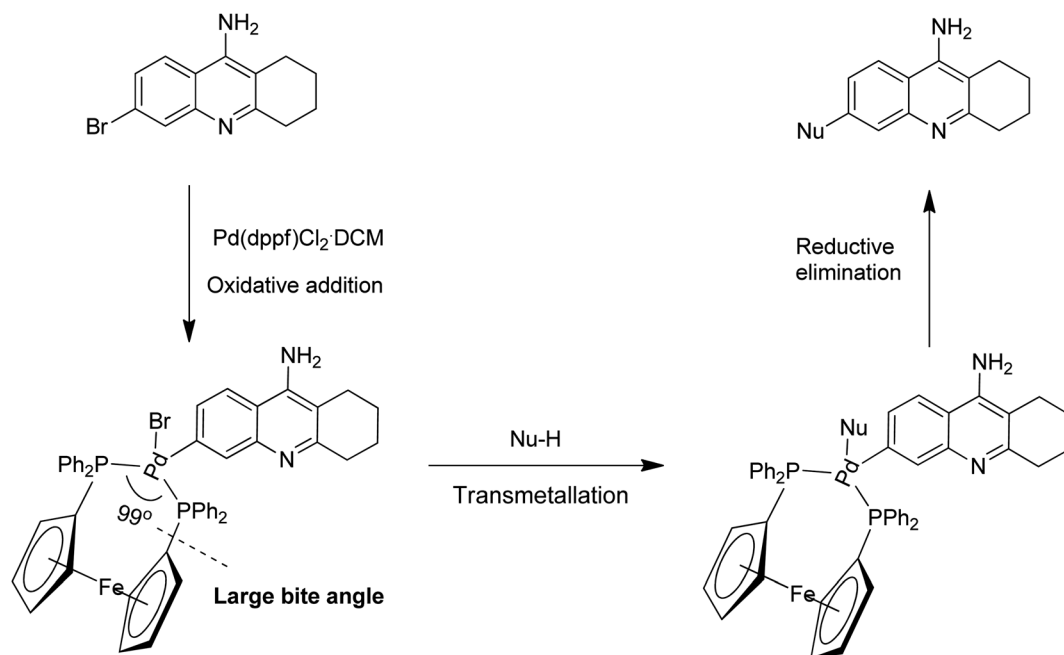
Scheme 8 Synthesis of 6-amino tacrine derivatives by Buchwald coupling; reaction conditions: 6-bromo tacrine (1 mmol), amine (1.3 mmol), Pd(dppf)Cl₂·CH₂Cl₂ (5 mol%), KOt-Bu (4 mmol), 1,4-dioxane (2 mL), 100 °C for 8–10 h.

The success of borylation and Suzuki–Miyaura cross-coupling reactions for the synthesis of novel tacrine analogues enlightened us to further explore the 6-bromo tacrine scaffold. We hypothesized that the 6-bromo tacrine **1** can be directly subjected to Suzuki–Miyaura cross-coupling conditions with different boronic acids in our previously optimized protocol. To substantiate this hypothesis, we treated the scaffold **1** with a series of boronic acids **5a–e** by employing Pd(dppf)Cl₂·CH₂Cl₂ as the catalyst, K₂CO₃ as base and 1,4-dioxane/H₂O (2 : 1) as the solvent system at 100 °C for 8–10 hours (Scheme 4). To our delight, we obtained the desired products **7a–e** in good to excellent yields (78–87%). The boronic acids bearing electron donating groups afforded the required products (**7d**, **7e**) in good yields whereas the boronic acids possessing electron

withdrawing groups yielded the desired products (**7a–c**) in excellent yields. The Suzuki–Miyaura cross-coupling methodology of 6-bromo tacrine scaffold with boronic acids was found to be slightly better than that of 6-borylated tacrine derivative (with aryl bromides) in terms of isolated yield of the obtained products.

Our next attention was to optimize the developed methodology for Stille cross-coupling conditions. Taking this into consideration, we treated the 6-bromo tacrine **1** with tributyl(4-methoxyphenyl)stannane **6d** in our developed protocol. Unfortunately, we obtained the desired product **7d** in slightly lesser yield at this time (Table 2, entry 1). We carried out the optimization studies by screening different solvent systems and bases/additives (Table 2). Gratifyingly, we found better yield of the required





Scheme 9 Proposed catalytic steps describing the ideality of $\text{Pd(dppf)Cl}_2 \cdot \text{CH}_2\text{Cl}_2$ catalyst.

product when the reaction was carried out in DMF (Table 2, entries 4–8). Finally, we got the expected product in 80% isolated yield when NaCl was employed as an additive (Table 2, entry 8). Even though the actual role of NaCl is unclear in the outcome of this reaction, it is speculated to undergo halide exchange with the oxidative adduct complex before the transmetalation step.

After optimizing the reaction conditions for Stille coupling, we decided to evaluate the substrate scope of this developed protocol (Scheme 5). Accordingly, we synthesized different 6-substituted tacrine analogues **7d–h** successfully in good to excellent yields (70–88%). The products **7d** and **7e** was also obtained in good yields by Suzuki–Miyaura coupling conditions. However, considering the toxicity of the stannanes, it is worth noting that the optimized reaction conditions for Stille coupling could be employed to those substrates (**7f–h**) which are difficult to obtain *via* corresponding Suzuki coupling reactions.

Our next attention was to optimize the reaction conditions for Sonogashira cross-coupling reactions of 6-bromo tacrine by employing $\text{Pd(dppf)Cl}_2 \cdot \text{CH}_2\text{Cl}_2$ as the catalyst. As Sonogashira cross-coupling is generally facilitated by copper salts and Hunig-bases,¹⁰ we decided to optimize the reaction conditions using copper iodide (CuI) and triethylamine (TEA). Accordingly, we carried out the cross-coupling reaction of 6-bromo tacrine **1** with various terminal acetylenes **8a–d** in CuI and TEA at 100°C for 8–10 hours (Scheme 6). Gratifyingly, we obtained the expected products in good to excellent yields (78–88%). The phenyl acetylenes bearing *para* substitution (**8a**, **8c**) procured the desired 6-alkynyl tacrines in excellent yields (84–88%) whereas acetylenes containing heteroaryl (pyridine) group yielded the expected product **9d** in good yield (78%).

The success of our trials in Suzuki–Miyaura, Sonogashira and Stille cross-couplings enlightened us about the special ability of

$\text{Pd(dppf)Cl}_2 \cdot \text{CH}_2\text{Cl}_2$ to act as a common catalyst in palladium catalyzed cross-coupling reactions of 6-bromo tacrine. This observation directed us to investigate the efficiency of this catalyst in Heck and Buchwald cross-coupling conditions.

Accordingly, we treated 6-bromo tacrine **1** with methyl acrylate **10a** in order to optimize the suitable conditions for Heck reaction using $\text{Pd(dppf)Cl}_2 \cdot \text{CH}_2\text{Cl}_2$ as the catalyst (Table 3). After careful screening of the reaction parameters, we obtained the desired product **11a** in 77% isolated yield when the reaction was carried out in DMF at 100°C (Table 3, entry 9). It is worth noting that the utilization of an organic base was a key factor for the success of this developed methodology (Table 3, entries 9 and 10).

After obtaining the suitable reaction conditions in hand, we evaluated the substrate scope of the developed methodology by synthesizing a variety of 6-alkenyl tacrine derivatives (Scheme 7). To our delight, all the alkenes reacted well efficiently to procure the expected products **11a–d** in good to excellent yields (75–80%).

In order to check the feasibility of our common catalyst in Buchwald coupling, we treated the intermediate **1** with 4-methoxybenzylamine **12a**. The detailed optimization studies that we carried out have been summarized in Table 4.

After the careful screening of reaction parameters, we could obtain the desired product **13a** in 72% isolated yield (Table 4, entry 11). It is noteworthy that the reaction proceeded well when potassium *tert*-butoxide was employed as a base and no additional ligands were needed for the success of our developed protocol. After the successful optimization of reaction conditions, we evaluated the substrate scope of our methodology for Buchwald coupling (Scheme 8). Gratifyingly, a series of 6-amino tacrine derivatives **13a–g** were synthesized in good to excellent yields by our optimized protocol (68–80%).

Table 5 Predicted ADME and physicochemical properties

Entry	TPSA	WLOGP	GI absorption	BBB permeant	CYP1A2 inhibitor	CYP2C19 inhibitor	CYP2C9 inhibitor	CYP2D6 inhibitor	CYP3A4 inhibitor	Lipinski #violations	PAINS #alerts
7a	38,91	4, 93	High	Yes	Yes	Yes	No	Yes	Yes	0	0
7b	38,91	5, 49	High	Yes	Yes	Yes	No	No	Yes	1	0
7c	38,91	5, 02	High	Yes	Yes	Yes	No	No	Yes	0	0
7d	48,14	4, 38	High	Yes	Yes	Yes	No	Yes	Yes	0	0
7e	48, 14	4, 38	High	Yes	Yes	Yes	No	Yes	Yes	0	0
7f	48, 14	3, 71	High	Yes	Yes	Yes	No	Yes	No	0	0
7g	38, 91	3, 43	High	Yes	Yes	Yes	No	Yes	No	0	0
7h	51, 8	4, 33	High	Yes	Yes	Yes	No	Yes	Yes	0	0
9a	38, 91	4, 74	High	Yes	Yes	Yes	Yes	No	No	1	0
9b	38, 91	4, 84	High	Yes	Yes	Yes	Yes	No	No	1	0
9c	38, 91	4, 84	High	Yes	Yes	Yes	Yes	No	No	1	0
9d	51, 8	3, 58	High	Yes	Yes	Yes	Yes	No	Yes	0	0
11a	65, 21	2, 78	High	Yes	Yes	Yes	Yes	No	No	0	0
11b	65, 21	3, 17	High	Yes	Yes	Yes	Yes	Yes	No	0	0
11c	65, 21	3, 95	High	Yes	Yes	Yes	Yes	No	No	0	0
11d	38, 91	4, 66	High	Yes	Yes	Yes	No	Yes	No	0	0
13a	60, 17	3, 98	High	Yes	Yes	Yes	No	Yes	Yes	0	0
13b	50, 94	6, 14	High	No	Yes	Yes	No	Yes	Yes	0	0
13c	50, 94	6, 14	High	No	Yes	Yes	No	Yes	Yes	0	0
13d	50, 94	5, 09	High	Yes	Yes	Yes	No	Yes	Yes	0	0
13e	50, 94	4, 45	High	Yes	Yes	Yes	No	Yes	Yes	0	0
13f	42, 15	4, 47	High	Yes	Yes	Yes	No	Yes	Yes	0	0
13g	63, 83	4, 96	High	Yes	Yes	Yes	No	Yes	Yes	0	0

The efficiency of $\text{Pd}(\text{dppf})\text{Cl}_2 \cdot \text{CH}_2\text{Cl}_2$ as a common catalyst in all our successful trials encouraged us to rationalize its importance in the cross-coupling methodologies developed.¹¹

It is well-known that most of these cross-coupling reactions between (hetero)aryl halides and nucleophiles involve a series of fundamental steps that occur at the Pd-metal centre (*e.g.*

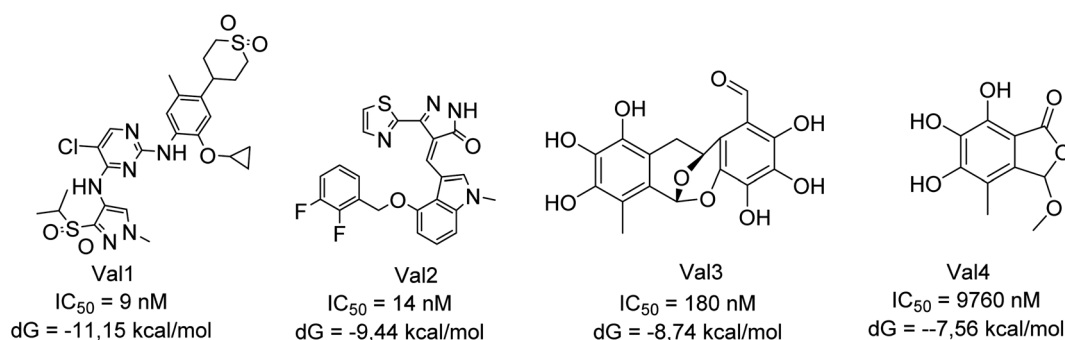


Fig. 1 Result of docking studies of known AChE inhibitors.



Table 6 Results of molecular docking studies

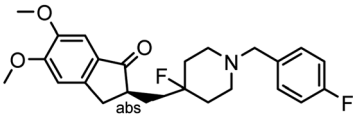
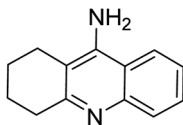
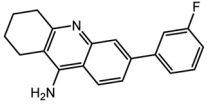
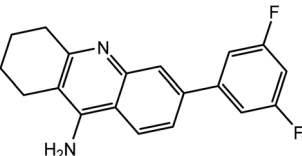
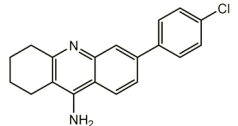
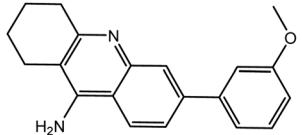
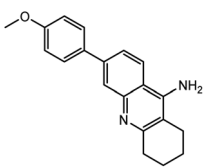
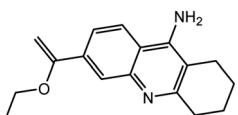
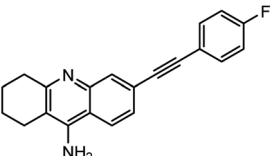
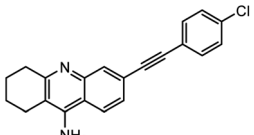
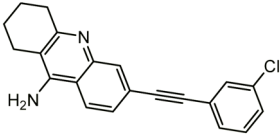
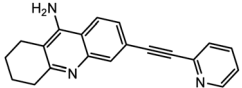
Compounds	Structures	Binding free energy, kcal mol ⁻¹		Reference
		7d9o	7e3i	
NL1		-12.55 (rmsd = 3 Å)	—	IC ₅₀ = 2.6 nM
Tacrine		—	-10.0, ..., -9.0 (rmsd = 2 Å)	IC ₅₀ = 105 nM
7a		-13.46	-13.54	
7b		-12.72	-12.60	
7c		-13.92	-13.67 (-12.41) ^a	
7d		-12.66	-12.77	
7e		-12.83	-12.95	
7f		-11.50	-11.71	
9a		-13.90	-11.91	
9b		-13.38	-11.83	



Table 6 (Contd.)

Compounds	Structures	Binding free energy, kcal mol ⁻¹		Reference
		7d9o	7e3i	
9c		-13.45	-14.95	
9d		-11.86	-11.20	

^a Recalculated position, close in position of the scaffold to tacrine. The most active compounds are marked in bold.

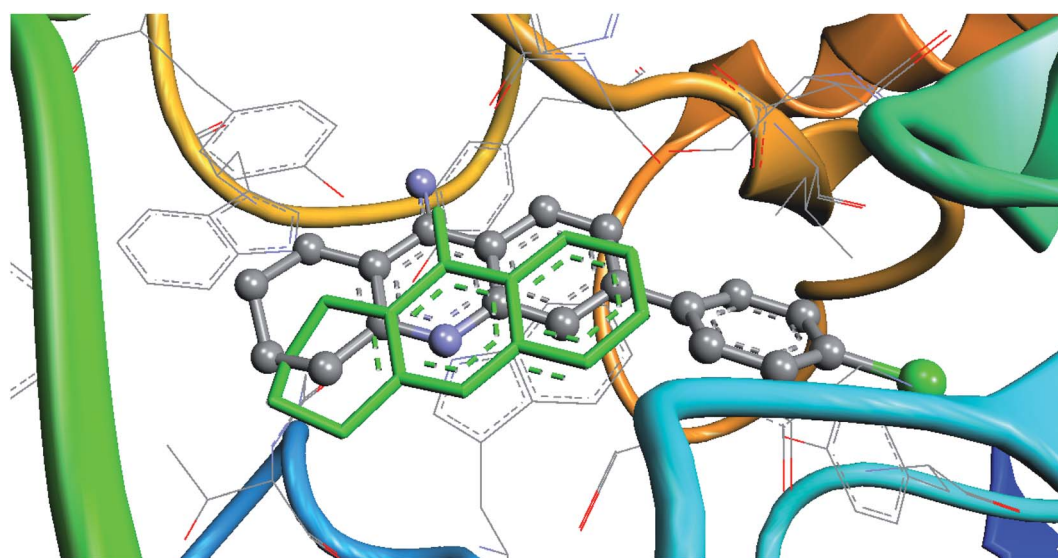


Fig. 2 Result of the redocking of compound 7c relative to tacrine (marked in green) in the 7e3i complex.

oxidative addition, coordination-insertion, transmetalation, association of nucleophile, reductive elimination *etc.*). Once the coordinatively unsaturated true catalytic species is generated, the electronic and steric properties encountered by this catalytic species play a pivotal role in enhancing the reaction rates of various steps involved in the catalytic cycle. Additionally, the steric and electronic properties of the electrophilic and nucleophilic coupling partners are also known to have an impact on the overall outcome of the process. The delicate balance between the steric and electronic parameters of Pd(dppf)Cl₂·CH₂Cl₂ when compared to other phosphine based bidentate catalytic systems is possibly the instrumental factor in achieving successful results in all these cross-coupling reactions employing a wide range of nucleophiles (Scheme 9). The following reasons are rationalized for the ideality of Pd(dppf)Cl₂·CH₂Cl₂ acting as a common catalyst:¹² (a) the facile generation of coordinatively unsaturated true catalytic species L₂Pd(0); (b) the true catalytic species undergoes rapid

oxidative addition; (c) the bidentate ligand attached provides excellent stability to the catalyst; (d) the larger bite angle (99.1 °C), smaller Cl–Pd–Cl angle and forced *cis* geometry of the groups to be eliminated enhances the reductive elimination step.

In silico studies

All the newly synthesized compounds were then subjected to *in silico* studies to get an understanding about their drug-likeness and pharmacological activities.

Prediction of ADME parameters

The SwissADME service¹³ was used to determine the key physicochemical and pharmacokinetic parameters of the studied compounds (Table 5). One of the key properties of AChE inhibitors is their ability to pass through the BBB (blood–brain–barrier). Only two compounds **13b** and **13c** do not meet this



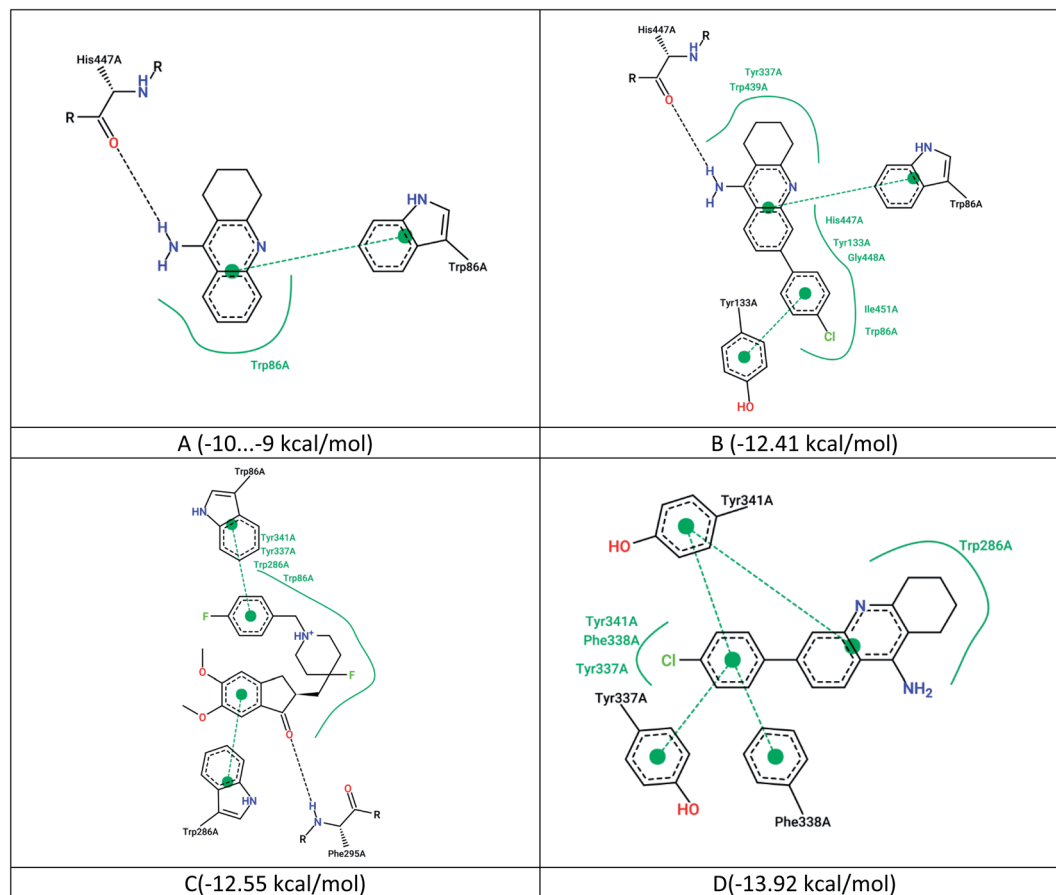


Fig. 3 2D maps of non-covalent interactions, (A) native ligand (tacrine) with $IC_{50} = 105$ nM; (B) ligand **7c** docked relative to tacrine (PDB 7e3i); (C) native nanomolar NL1 inhibitor with $IC_{50} = 2.6$ nM; (D) ligand **7c** docked to NL1 (PDB 7d9o).

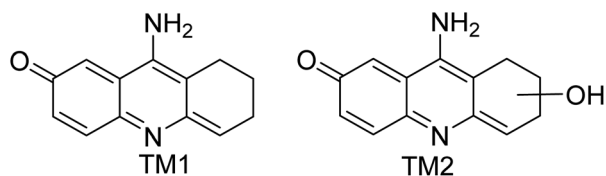


Fig. 4 Hepatotoxic metabolites of tacrine formed with the participation of CYP1A2.

criterion. Moreover, all the newly synthesized compounds successfully passed the PAINS filter.

In silico docking studies

Among the five known drugs for the therapy of Alzheimer's disease (AD), four of them (tacrine, donepezil, rivastigmine and galantamine) are inhibitors of acetylcholinesterase (AChE) enzyme.¹⁴ In view of this observation, we decided to carry out the molecular docking studies of the newly synthesized tacrine analogs (ligands) at the active site of AChE. The molecular docking studies were done by using ArgusLab and DataWarrior software *via* ArgusDock algorithm (+empirical evaluation function Ascore). As model compounds, AChE complex with

competitive inhibitor tacrine with $IC_{50} = 105$ nM (PDB ID 7e3i) and AChE complex with competitive NL1 inhibitor with $IC_{50} = 2.67$ nM (PDB ID 7d9o) were used. The validation results were carried out by redocking the native ligand and comparing the *in vitro/in silico* activity indicators of known AChE inhibitors (Fig. 1).

Molecular docking results

During the docking studies, we observed that almost all the ligands possessed lower values of binding free energy relative to the values for native ligands of various structures (tacrine and NL1). The compounds **7c** and **9c** have the highest calculated activity (Table 6). However, the compound **7c** was found to be the most active one in our investigation.

Analysis of non-covalent interactions

The most active compound **7c** (Table 6) was recalculated for AChE proteins from complexes "7d9o" and "7e3i". In the complex with tacrine (PDB 7e3i), ligand **7c** was redocked relative to the tacrine position (because they have a common scaffold). An example of redocking for this complex is shown in Fig. 2.

The maps of non-covalent interactions of native ligands and **7c** are presented in Fig. 3. As observed from Fig. 2, 3A and B, the



Table 7 Results of toxicity prediction of tacrine analogues by different approaches^a

Compounds	Docking score, kcal mol ⁻¹		LD ₅₀ (rat, intravenous route of administration//GUSAR model)
	CYP1A2	CYP3A4	
7,8-Benzoflavone (IC ₅₀ (1A2) = 340 nM)	−13.47	NA	NA
Ketoconazole IC ₅₀ (3A4) = 200 nM	NA	−10.49	NA
Tacrine	−10.9 IC ₅₀ = 1.5 μM	−9.8 IC ₅₀ = 97 μM	34.94 (real LD ₅₀ = 20 mg kg ⁻¹)
7a	−14.42	−10.27	61.38
7b	−14.24	−10.65	61.39
7c	−15.05	−15.36	51.65
7d	−13.54	−10.74	64.52
7e	−13.64	−10.19	72.60
7f	−11.38	−10.90	27.57
7g	−12.51	−12.05	35.07
7h	−12.33	−10.70	87.19
9a	−15.40	−12.0562	42.53
9b	−15.12	−10.25	42.76
9c	−16.00	−15.53	54.97
9d	−13.14	−12.12	65.00
11a	−11.71	−11.70	61.09
11b	−12.26	−10.99	33.17
11c	−12.10	−12.96	43.23
11d	−15.78	−14.54	68.72
13a	−11.44	−9.24	53.24
13b	−14.74	−12.38	57.81
13c	−14.08	−12.03	60.33
13d	−13.18	−13.32	44.53
13e	−13.38	−11.53	44.74
13f	−13.44	−12.97	35.89
13g	−12.65	−11.75	50.06

^a The most active compound is marked in bold; NA – not analyzed.

lead compound **7c** has a similar non-covalent interaction profile (hydrogen bonding to His447, π - π stacking to Trp86) and a lower binding energy relative to tacrine (probably due to additional van der Waals interactions and π - π stacking with Tyr133). However, there are more energetically favorable states for this ligand in the active site, which are completely inconsistent with the position of tacrine.

The results of redocking of ligand **7c** at the PDB 7d9o complex show a different profile of non-covalent interactions of the ligand relative to the nanomolar NL1 inhibitor (Fig. 3C and D). At the same time, the resulting complex with ligand **7c** is more stable due to the many stacking effects.

Toxicity prediction studies

Based on the high toxicity of tacrine, an important issue is the assessment of the acute toxicity of the proposed structural analogues as well as determining the stability of their complexes with CYP3A4 and CYP1A2 proteins. In general, these two proteins play a key role in the formation of hepatotoxic metabolites of tacrine (Fig. 4) and the metabolism of xenobiotics.¹⁵ Accordingly, our next attention was to predict the hepatotoxicity of the newly synthesized tacrine derivatives.

The acute toxicity studies of synthesized tacrine analogues were analyzed using the GUSAR service¹⁶ in a model of LD₅₀ prediction in rats administered intravenously. The potential hepatotoxicity of the ligands was assessed by docking against

complexes of CYP1A2 (PDB 2hi4) and CYP3A4 (PDB 2v0m) proteins with known inhibitors like 7,8-benzoflavone and ketoconazole respectively. The proteins were prepared in the same way as for AChE. The size of binding sites was calculated relative to native ligands. Docking was carried out in Arguslab using the same algorithm and settings as before. To validate the protocol, redocking of native ligands was carried out with the following results: 7,8-benzoflavone - RMSD = 1.42 Å, G = 13.47 kcal mol⁻¹, ketoconazole - RMSD = 1.22 Å, ΔG = −10.49 kcal mol⁻¹. The results of docking and calculation of acute toxicity by the GUSAR regression model are shown in Table 7.

The results of the GUSAR regression model show that all derivatives, with the exception of **7f**, have less acute toxicity (when administered intravenously to rats) compared to the predicted value for tacrine. On average, the lowest toxicity is predicted for 6-aryl-substituted derivatives **7a-h** (average LD₅₀ = 62 mg kg⁻¹) in comparison with compounds having alkyne fragment **9a-d** (average LD₅₀ = 51 mg kg⁻¹) as linkers. The high predicted acute toxicity of compound **7f** appears to be related to the reactivity of the ethylene moiety.

As reported by Rao *et al.*¹⁵ the pathways of tacrine metabolism are directly related to the way it is oriented relative to the heme in CYP1A2. Thus, the proximity of the tetrahydrobenzene fragment of tacrine to heme leads to its enzymatic hydroxylation. Similar positioning of the studied tacrine analogues was



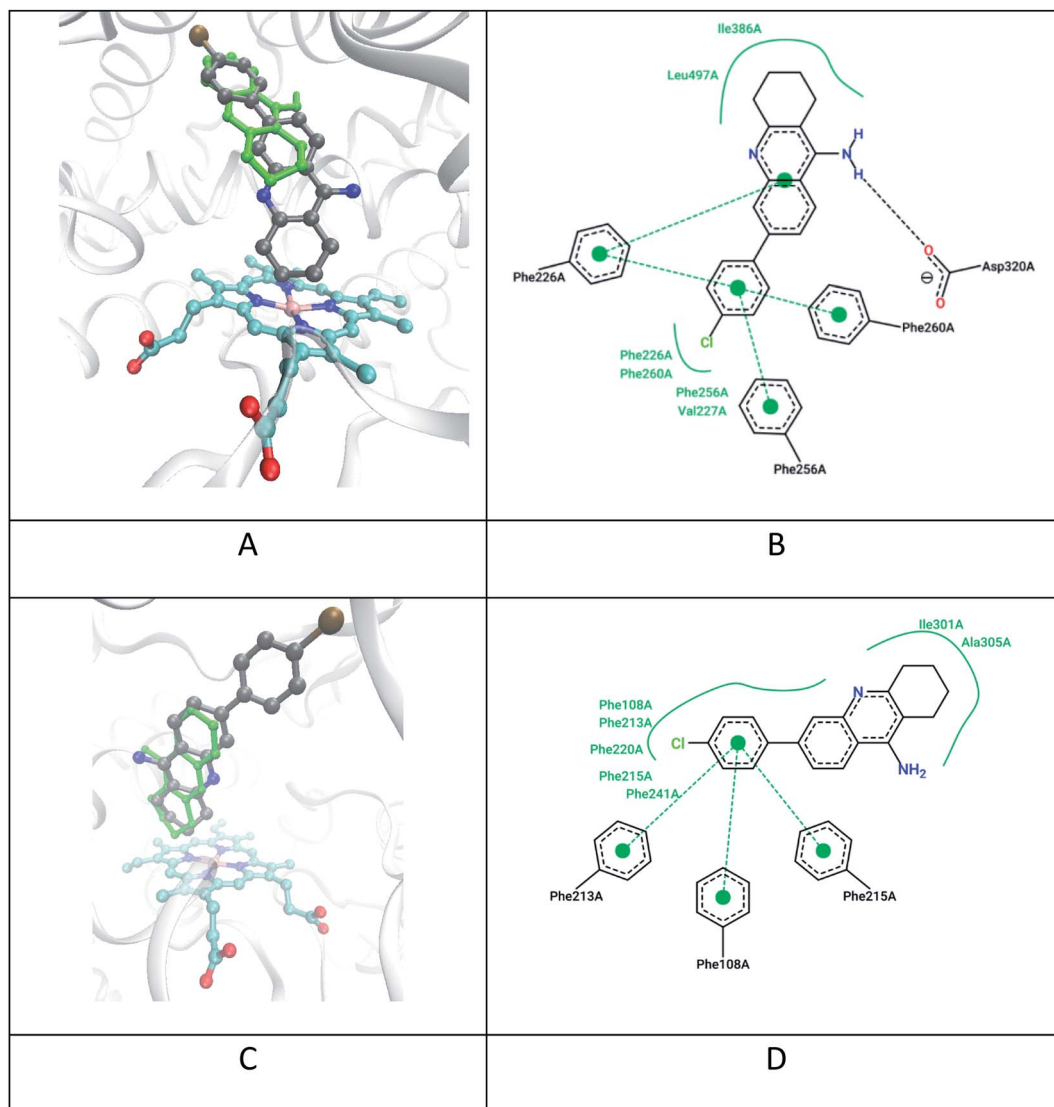


Fig. 5 Docking results of the compound **7c** and tacrine for CYP1A2 and CYP3A4 subtype proteins: (A) positions **7c** (grey), tacrine (green), heme (cyan) in CYP1A2 (PDB 2hi4); (B) 2D map of non-covalent interactions of **7c** in CYP1A2; (C) calculated positions **7c** (grey), tacrine (green), heme (cyan) in CYP3A4 (PDB 2v0m); (D) 2D map of non-covalent interactions of **7c** in CYP3A4.

established as a result of docking on CYP1A2 and CYP3A4 (Fig. 5).

All ligands show high potential affinity for CYP1A2 (to a greater extent) and CYP3A4 (to a lesser extent). Also, the ligands with highest affinity are characterized by the close location of the tetrahydroacridine fragment of the ligands to heme which contributes to their enzymatic hydroxylation. For example, the distance between the nearest carbon atom of the tetrahydroacridine fragment of ligand **7c** and the heme “Fe” ion is about 4.3 Å in CYP1A2 (Fig. 5A) and 5.5 Å in CYP3A4 (Fig. 5C). However, the further metabolism of ligands at the C-7 with the formation of analogues of hepatotoxic metabolites (Fig. 5) can be sterically hampered in the presence of a large substituent at C-6 position of **7c**.

Similarly, an aromatic fragment at C-6 can lead to an alternative ligand approach to heme in CYP1A2 and CYP3A4

enzymes. For example, the compound **7e**, with the least predicted acute toxicity, orients itself in the CYP1A2 enzyme with the aromatic substituent approaching the heme “Fe” ion at a distance of ~5.3 Å (Fig. 6) with further metabolism without the participation of the tetrahydroacridine.

Thus, as a result of the virtual screening of newly synthesized tacrine compounds by molecular docking, their high inhibitory activity against AChE was established relative to the nanomolar inhibitor – tacrine with a similar profile of non-covalent interactions. Most of the compounds also exhibited 1.5–2 times lower predicted acute toxicity according to the GUSAR model. A high affinity of the compounds for the CYP1A2 enzyme, which plays a key role in tacrine metabolism, has also been established. For the studied derivatives, 2 possible ways of binding to CYP1A2 were established: (1) with the maximum approximation to the heme of the tetrahydroacridine fragment with the

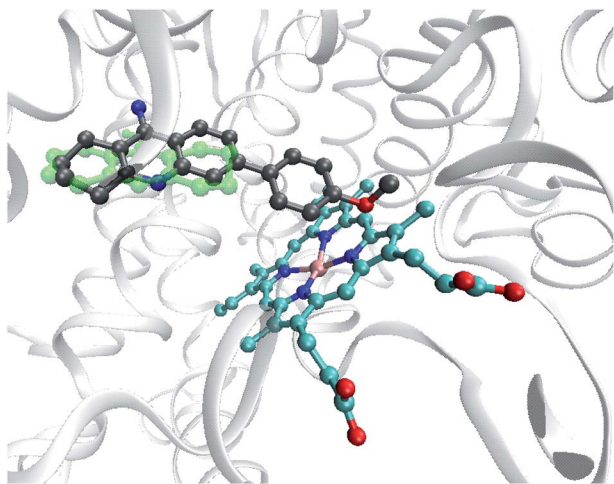


Fig. 6 The results of the docking studies for the compound **7e** (grey) and tacrine (green) on the CYP1A2 protein with the closest location of the aromatic substituent to heme (cyan).

possibility of its enzymatic hydroxylation; (2) as close as possible to the heme of the aromatic substituent at the “C-6” of the ligand with its further metabolic transformation, thus preventing the metabolism of the tetrahydroacridine ring to probable hepatotoxic derivatives.

Conclusion

We have successfully demonstrated the utilization of $\text{Pd}(\text{dppf})\text{Cl}_2 \cdot \text{CH}_2\text{Cl}_2$ as a common catalyst for the palladium catalyzed cross-coupling reactions of 6-bromo tacrine with various coupling partners. The developed methodologies paved the way for the successful synthesis of diverse array of 6-substituted tacrine analogues of profound pharmacological relevance. The molecular docking and hepatotoxicity prediction studies were carried out for the synthesized compounds. From our studies, we found that most of the synthesized compounds are active as they possessed appreciable binding energy and low toxicity values. The compound **7c** showed the highest calculated activity in relative to tacrine when docked at the active site of AChE enzyme. The hepatotoxicity prediction studies revealed the fact that the compound **7e** had the least predicted acute toxicity. The synthesis of additional compounds and the evaluation of their biological activities will be carried out in our laboratory in due course.

Conflicts of interest

The authors declare no conflicts of interest.

Acknowledgements

Aravinda Babu is thankful to Syngene International Ltd. for providing the No Objection Certificate (NOC) to pursue his doctoral work. The authors are thankful to Sri Siddhartha Academy of Higher Education and Karnataka Council for

Technological Upgradation (KCTU) for rendering all the facilities to carry out the research work. Grigory V. Zyryanov is thankful to Ministry of Science and Higher Education of the Russian Federation (Grant # 075-15-2020-777) for the financial support. Sougata Santra is thankful to Russian Science Foundation (Grant # 20-73-10205) and Grants Council of the President of the Russian Federation (# NSH-1223.2022.1.3). Muthipeedika Nibin Joy is thankful to Russian Science Foundation (Grants ## 22-23-20189 and 21-13-00304). The detailed experimental procedure and characterization data including spectra are available in the ESI† uploaded along with the manuscript.

References

- H. Wang and H. Zhang, *ACS Chem. Neurosci.*, 2019, **10**, 852–862.
- X. j. Cheng, J. x. Gu, Y. p. Pang, J. Liu, T. Xu, X. r. Li, Y. Z. Hua, K. A. Newell, X. F. Huang, Y. Yu and Y. Liu, *ACS Chem. Neurosci.*, 2019, **10**, 3500–3509.
- L. Ismaili, B. Refouvelet, M. Benchekroun, S. Brogi, M. Brindisi, S. Gemma, G. Campiani, S. Filipic, D. Agbaba, G. Esteban, M. Unzeta, K. Nikolic, S. Butini and J. M. Contelles, *Prog. Neurobiol.*, 2017, **151**, 4–34.
- (a) L. Gorecki, A. Misiachna, J. Damborsky, R. Dolezal, *et al.*, *Eur. J. Med. Chem.*, 2021, **219**, 113434; (b) W. Liu, L. Wu, D. Li, Y. Huang, *et al.*, *Bioorg. Chem.*, 2022, **126**, 105875; (c) M. Recanatini, A. Cavalli, F. Belluti, L. Piazzzi, *et al.*, *J. Med. Chem.*, 2000, **43**, 2007–2018; (d) F. Mao, J. Li, H. Wei, L. Huang and X. Li, *J. Enzyme Inhib. Med. Chem.*, 2015, **30**, 995–1001.
- (a) M. A. Rajendra, K. Sunil, A. M. Sajith, M. N. Joy, V. A. Bakulev and K. R. Haridas, *Synlett*, 2020, **31**, 1629–1633; (b) S. Bhaskaran, M. S. A. Padusha and A. M. Sajith, *ChemistrySelect*, 2020, **5**, 9005–9016.
- (a) R. P. Karuvalam, K. R. Haridas, A. M. Sajith, R. Pakkath, B. Savitha, M. S. A. Padusha, V. A. Bakulev and M. N. Joy, *Arkivoc*, 2019, **6**, 431–445; (b) B. Savitha, E. K. Reddy, C. S. A. Kumar, R. P. Karuvalam, M. S. A. Padusha, V. A. Bakulev, K. H. Narasimhamurthy, A. M. Sajith and M. N. Joy, *Tetrahedron Lett.*, 2019, **60**, 151332.
- (a) E. K. Reddy, C. Remya, K. Mantosh, A. M. Sajith, R. V. Omkumar, C. Sadasivan and S. Anwar, *Eur. J. Med. Chem.*, 2017, **139**, 367–377; (b) C. Remya, K. V. Dileep, E. K. Reddy, K. Mantosh, K. Lakshmi, R. S. Jacob, A. M. Sajith, E. J. Variyar, S. Anwar, K. Y. J. Zhang, C. Sadasivan and R. V. Omkumar, *Comput. Struct. Biotechnol. J.*, 2021, **19**, 4517–4537.
- (a) D. Alberico, M. E. Scott and M. Lautens, *Chem. Rev.*, 2007, **107**, 174–238; (b) F. Bellina and R. Rossi, *Tetrahedron*, 2009, **65**, 10269–10310.
- (a) G. P. McGlacken and L. M. Bateman, *Chem. Soc. Rev.*, 2009, **38**, 2447–2464; (b) L. Ackermann, R. Vicente and A. R. Kapdi, *Angew. Chem., Int. Ed.*, 2009, **48**, 9792–9826.
- R. Chinchilla and C. Najera, *Chem. Rev.*, 2007, **107**, 874–922.
- P. G. Gildner and T. J. Colacot, *Organometallics*, 2015, **34**, 5497–5508.



- 12 T. J. Colacot, *Platinum Met. Rev.*, 2001, **45**, 22–30.
- 13 A. Daina, O. Michielin and V. Zoete, *Sci. Rep.*, 2017, **7**, 42717.
- 14 P. Camps, X. Formosa, C. Galdeano, T. Gómez, D. Muñoz-Torrero, L. Ramírez, E. Viayna, E. Gómez, N. Isambert, R. Lavilla, A. Badia, M. V. Clos, M. Bartolini, F. Mancini, V. Andrisano, A. Bidon-Chanal, O. Huertas, T. Dafni and J. Luque, *Chem.-Biol. Interact.*, 2010, **187**, 411–415.
- 15 A. McEneny-King, W. Osman, A. N. Edginton and P. P. N. Rao, *Bioorg. Med. Chem. Lett.*, 2017, **27**, 2443–2449.
- 16 A. Lagunin, A. Zakharov, D. Filimonov and V. Poroikov, *Mol. Inf.*, 2011, **30**, 241–250.

